

**FUNCTIONAL ANALYSIS OF THE EXTRACELLULAR CYSTEINE RESIDUES
IN THE HUMAN ORGANIC ANION TRANSPORTING POLYPEPTIDE,
OATP2B1**

**Emanuel Hänggi¹, Anne Freimoser Grundschober¹, Simone Leuthold,
Peter J. Meier and Marie V. St-Pierre**

**From the Division of Clinical Pharmacology and Toxicology, Department of
Medicine, University Hospital Zürich, Zürich, Switzerland**

Running title: Function of extracellular cysteines in the OATP2B1 transporter

Address correspondence to:

Marie V. St-Pierre,
Division of Clinical Pharmacology and Toxicology,
University Hospital Zürich,
100 Rämistrasse, Zürich 8091, Switzerland,
Tel: ++41 (0) 44 255-9456;
E-Mail: stpierre@kpt.unizh.ch

Number text pages: 34

Number tables: 1

Number figures: 12

Number references: 25

Words in Abstract: 227

Words in Introduction: 480

Words in Discussion: 1479

Abbreviations: OATP, organic anion transporting polypeptide; MTSEA, *N*-biotinoylaminoethyl methanethiosulfonate; PNGaseF, peptide N-glycosidase F; DTSSP, 3,3'-Dithiobis-[sulfosuccinimidylpropionate]; BS³, Bis-[sulfosuccinimidyl]-suberate; DHEAS, dehydroepiandrosterone sulfate; Sulfo-NHS-LC-Biotin, sulfonated N-hydroxysuccinimide; DAPI, 4'-6-diamidino-2-phenylindole; ALLN, N-acetyl-L-leucyl-L-leucyl-L-norleucinal

ABSTRACT

Organic Anion Transporting Polypeptide (OATP) superfamily member 2B1 (OATP2B1) mediates the uptake of steroid hormone precursors and selected drugs in the placenta, liver, mammary gland, brain and intestine. This action is modulated by sulfhydryl reagents. Common to all OATPs is a large extracellular loop between transmembrane domains IX and X with ten conserved cysteines. To elucidate the structure-function relationship of this cysteine rich ectodomain, a truncated OATP2B1 lacking ten extracellular cysteines (OATP2B1 $_{\Delta 489-557}$) and ten OATP2B1 mutants containing individual Cys to Ala substitutions were generated and expressed in CHO-K1 cells. The immunolocalization, cell-surface expression, transport activity and free cysteine labeling with *N*-biotinoylaminoethylmethanethiosulfonate (MTSEA) of mutant proteins and wild-type OATP2B1 were compared. OATP2B1 $_{\Delta 489-557}$ accumulated intracellularly. Nine Cys to Ala substitutions, C489A, C495A, C504A, C516A, C520A, C539A, C541A, C553A and C557A were misprocessed, appearing predominantly as core-glycosylated, 60 kDa proteins and as 180 kDa complexes. Only C493A was a fully-glycosylated, 75 kDa protein expressed at the cell surface. Thapsigargin partially corrected the misprocessing of mutants. Compared to OATP2B1, C493A and C557A transported estrone-3-sulfate and dehydroepiandrosterone sulfate less efficiently, whereas all others mutants were functionally impaired. MTSEA labeled free cysteines in all Cys to Ala mutants but not in OATP2B1, suggesting that all ten extracellular cysteines are normally disulfide-bonded. Our findings show that the trafficking and function of OATP2B1 is vulnerable to changes in the cysteine residues of extracellular loop IX-X.

The Organic Anion Transporting Polypeptides (humans: OATPs, rodents: Oatps) are gene products of the solute carrier gene superfamily, *SLCO* (Hagenbuch and Meier, 2004). These multispecific, sodium-independent solute carriers mediate the cellular uptake of a range of amphipathic endogenous and exogenous molecules (Hagenbuch and Meier, 2004). OATP family member 2B1 (OATP2B1; gene symbol, *SLCO2B1*) is expressed at the basolateral membrane of hepatocytes (Kullak-Ublick et al., 2001), the basal surface of the placental syncytiotrophoblast (St-Pierre et al., 2002), the apical membrane of enterocytes (Kobayashi et al., 2003), as well as in the mammary gland (Pizzagalli et al., 2003) and in the ciliary body of the eye (Gao et al., 2005). When uptake experiments are conducted at a neutral pH, OATP2B1 mediates the transport of the natural steroid conjugates, estrone-3-sulfate and dehydroepiandrosterone sulfate (DHEAS) (Pizzagalli et al., 2003), and the hypoglycemic drug, glibenclamide (Sato et al., 2005). At an acidic pH, such as exists in the small intestine, the substrate specificity of OATP2B1 broadens to include taurocholate and the drugs, pravastatin and fexofenadine (Kobayashi et al., 2003; Nozawa et al., 2004). Hydrophathy analysis predicts that the secondary structure of OATP2B1 conforms to the pattern described for all OATP/Oatp family members, that is 12 transmembrane helices, cytoplasmic oriented N- and C-termini, and a large extracellular loop between transmembrane domains IX and X that contains 10 conserved cysteine residues (Hagenbuch and Meier, 2004). In the case of the 709-amino acid OATP2B1 protein, the large extracellular loop is comprised of 94 residues with cysteines at positions C489, C493, C495, C504, C516, C520, C539, C541, C553 and C557 (Figure 1). The structure-function relationship of this extracellular loop with its multiple, conserved cysteines is not known, despite the fact that all OATP/Oatp proteins share this structural motif. What is known is that cysteine residues are likely involved in substrate binding and/or transport because estrone-3-sulfate uptake is sensitive to both the lipophilic and hydrophilic thiol reagents, N-

ethylmaleimide and acetamido-4'-(iodoacetyl)amino-stilbene-2,2'-disulfonic acid, respectively (Pizzagalli et al., 2003). These observations give rise to the hypothesis that one or more of the invariant cysteines is susceptible to sulfhydryl modification, that this modification could alter the structure or function of OATP2B1, and that all OATP/Oatp proteins would be similarly affected.

The aim of the present work was to investigate the structure-function relationship of the conserved cysteine residues within the extracellular IX-X loop of OATP2B1. First, in order to gauge the importance of the entire extracellular IX-X loop, a truncated OATP2B1 protein was designed that harbored a deletion of all 10 extracellular cysteines as well as the intervening sequence (OATP2B1 $_{\Delta 489-557}$). In a second set of experiments, the invariant extracellular Cys residues were individually mutated to Ala to create a series of 10 mutant proteins with the extracellular loop otherwise intact. The functional consequences of the C489A, C493A, C495A, C504A, C516A, C520A, C539A, C541A, C553A and C557A substitutions were then examined and compared with wild-type OATP2B1.

MATERIALS AND METHODS

Cloning and mutagenesis of human OATP2B1. The open reading frame of the OATP2B1 cDNA was ligated into the PmeI sites of the pcDNA5/FRT vector (Invitrogen, Carlsbad, CA). A truncated OATP2B1 $_{\Delta 489-557}$, bearing a deletion of 69 amino acids from extracellular loop IX-X that includes all 10 conserved Cys residues, was generated using overlap extension PCR (Horton et al., 1993). Briefly, two fragments flanking the desired deletion were amplified by PCR separately: fragment 1 with forward primer f1 (5'-TGGCGTCCTGGTCAAGCGGCTCC-3') and reverse primer r2 (5'-ACCACCAGATGGCTGCTTGGAGACAGCTCCAGCCC-3') resulted in an amplicon upstream of the planned deletion; fragment 2 with forward primer f3 (5'-AGCTGTCTCCAAGCAGCCATCTGGTGGTGCCCTTCCT-3') and reverse primer r4 (5'-GTTTCGGAGCAGGTCATTATTGTAGTAGCGA-3') resulted in an amplicon downstream of the planned deletion. The two PCR fragments annealed to form a template in a second round of PCR with primers f1 and r4. The region spanning bases 1465-1671, which included the bases coding for all 10 conserved Cys, was deleted from the final amplicon. This amplicon was cloned into the pCMV6-XL5 vector (Origene, Rockville MD) then digested at two internal ApaI restriction sites to excise a fragment that was ligated into the cDNA of OATP2B1, which had also been digested at two internal ApaI restriction sites to excise a 577 bp fragment corresponding to the large extracellular loop. The exchange of these two fragments created the cDNA for the truncated OATP2B1 $_{\Delta 489-557}$ protein. For mutagenesis of individual Cys residues, the 577 bp ApaI digested fragment coding for the extracellular loop of OATP2B1 was ligated into the pBluescript vector. Point mutations were introduced using the QuikChange® Mutagenesis Kit (Stratagene, La Jolla, CA) to substitute, in turn, each of the 10 conserved cysteines at positions C489, C493, C495, C504, C516, C520, C539, C541, C553 and C557 with alanine. The ApaI fragment was then exchanged with the

corresponding fragment in wild-type OATP2B1. DNA sequencing confirmed the presence of the desired mutations.

Two tagged OATP2B1 proteins were designed for use in cross-linking experiments. A hemagglutinin A (HA) epitope tag or a 6X histidine epitope tag were added to the amino-terminal end of wild-type OATP2B1 cDNA by PCR. To generate the HA-OATP2B1 construct, the forward primer was 5'-GCGAATTCACCATGGCTTACCCATACGACGTCCCAGACTACGCTGGACCCAGGATAGGGCCAGCGG-3' and the reverse primer was 5'-GGGCGGCCGCTCACACTCGGGAATCCTCTGGC-3'. To generate the 6X His-OATP2B1 construct, the same reverse primer was paired with the forward primer, 5'-GCAAGCTTACCATGGCTCACCACCACCACCACCGGACCCAGGATAGGGCCAGCGG-3'. The HA-OATP2B1 PCR product (2200 bp) was gel purified, digested with EcoRI and NotI and ligated into the pIRESneo2 vector (Invitrogen). The His-OATP2B1 PCR product was digested with HindIII and NotI and ligated into the vector pcDNA5/FRT. The DNA sequences of both constructs were verified by sequencing.

Stable expression of OATP2B1 in CHO-K1 cells. Stable cell lines were generated using the Flp recombinase-mediated system, which permits the targeted integration of genes to the same locus in all transfected cells to provide a homogeneous level of gene expression. Flp-In™ Chinese Hamster Ovary host cells (CHO-K1) (Invitrogen) were cultured in F-12 nutrient media supplemented with 10% fetal calf serum, 2mM L-glutamine, and 100 µg/ml zeocin (Gibco Invitrogen, Paisley, Scotland) at 37°C with 5% CO₂. Cells were transfected with the pcDNA5/FRT expression vector containing the OATP2B1 or the 6X His-OATP2B1 constructs and the plasmid pOG44 that encodes the Flp recombinase by treatment with Lipofectamine 2000 (Invitrogen). Stably transfected cells were selected in 500 µg/ml hygromycin. Control cells were transfected with the pcDNA5/FRT vector without insert. HA-OATP2B1 in pIRESneo2 was transfected into Flp-In™ CHO-K1 cells without pOG44

and stable transfectants were selected in 500 $\mu\text{g/ml}$ geneticin. To obtain double transfectants, HA-OATP2B1 in pIRESneo2 was transfected into stably expressing His-OATP2B1 Flp-In™ CHO-K1 cells without pOG244, and selected in hygromycin and geneticin. Crude membranes were prepared from each cell line as described (Pizzagalli et al., 2003) and analyzed by Western blotting.

Cell Surface Biotinylation. Cell-surface proteins were biotinylated with either sulfonated N-hydroxysuccinimide biotin (Sulfo-NHS-LC-Biotin) (Pierce, Rockford, IL) or *N*-biotinoylaminoethyl methanethiosulfonate (MTSEA-Biotin) (Toronto Research Chemicals, Toronto, Canada). The cell-impermeant Sulfo-NHS-LC-Biotin reacts with primary amines and was used to estimate the plasma membrane expression of wild-type and mutant OATP2B1 proteins. MTSEA-Biotin reacts only with cysteinyl sulfhydryl groups and was used to assess the availability of free cysteines within the extracellular loops of OATP2B1 at the cell surface. Transfected CHO-K1 cells were grown to 75% confluence in 10-cm plates and were washed twice with ice-cold PBS supplemented with 1 mM MgCl_2 and 0.1 mM CaCl_2 , then incubated with biotinylation agent (Sulfo-NHS-LC-Biotin (0.5 mg/ml) or MTSEA-Biotin (300 μM)) for 20 min in PBS- $\text{Ca}^{2+}/\text{Mg}^{2+}$ at 4°C. Unbound Sulfo-NHS-LC-biotin or MTSEA-biotin in the reaction was quenched in 100 mM glycine or 50 mM NH_4Cl , respectively. Cells were washed twice in 25 mM Tris, 0.15 M NaCl , pH 7.2 (TBS) then incubated with constant agitation at 4°C in 500 μl lysis buffer (150 mM NaCl, 5 mM EDTA, 1% Triton X-100, 0.1 % BSA, 20 mM octyl glucoside, 10 mM Tris-Cl, pH 7) containing protease inhibitors for 30 min. After centrifugation at 10 000 x *g* for 2 min, 400 μl of the cell lysate were added to 400 μl of a neutravidin-bead suspension in mini-spin columns (Pierce). The remaining lysate (100 μl) was stored at -80°C. Spin columns were rotated for 1 h at room temperature to allow binding of neutravidin and biotinylated proteins. The beads were washed three times (150 mM NaCl, 5 mM EDTA, 1% Triton X-100, 1% sodium

deoxycholate, 10 mM Tris-Cl, pH 7) before elution of the biotinylated proteins with 400 μ l sample buffer (62.5 mM Tris-Cl, pH 6.8, 1% SDS, 10% glycerol) containing 75 mM DTT and protease inhibitors for 1 h at room temperature. The beads were pelleted for 2 min at 1000 \times g and bromophenol blue was mixed with the supernatant before SDS-PAGE electrophoresis and Western blotting.

Thapsigargin treatment and Western-blot analysis. In order to improve the cell surface expression of mutant OATP2B1 proteins (Egan et al., 2002), separate experiments were conducted where cells were treated with the calcium pump inhibitor, thapsigargin (Alexis Biochemicals, Lausen, Switzerland), prior to cell surface biotinylation, transport or immunofluorescence studies. Subconfluent cells were treated with thapsigargin 1 μ M for 1.5 h at 37°C in F-12 medium without antibiotics then allowed to recover for 2 h. For Western blotting, proteins in cell lysates or membrane preparations were separated by SDS-PAGE on 7.5% gels and transferred onto nitrocellulose membrane and immunodetected with a polyclonal rabbit antibody raised against the C-terminus of OATP2B1 as described (Pizzagalli et al., 2003). The endoplasmic reticulum heat shock 70 protein, GRP78 (BiP), was detected in cell lysates using a polyclonal rabbit antibody (Alexis Biochemicals) at 2 μ g/ml. Scanning densitometry was performed on a Kodak Image Station 2000MM analyzer (Eastman Kodak Co., Rochester, NY).

Deglycosylation assays. Enzymatic deglycosylation was performed with peptide N-glycosidase F (PNGase F) (Sigma-Aldrich Chemie, Buchs, Switzerland) or with endoglycosidase H (New England Biolabs, Ipswich, MA). Crude membrane preparations (30 μ g protein) were pre-incubated in denaturation buffer containing protease inhibitors for 2

h at 37°C, prior to the addition of PNGase F or endoglycosidase H for 12-15 h at 37°C. Control reactions were performed in the absence of enzymes. In a separate experiment, OATP2B1 transfected cells were incubated for 15 h with tunicamycin (3 µg/ml) (Fluka, Buchs, Switzerland) to inhibit glycosylation.

Immunofluorescent detection of OATP2B1 in transfected cells. CHO-K1 cells that stably expressed wild-type and mutant OATP2B1 were grown on glass coverslips and fixed in 4% paraformaldehyde. Cells were processed for confocal laser scanning microscopy (Leica Microsystems, Glattbrugg, Switzerland) by incubating with an affinity purified rabbit OATP2B1 antiserum and a Cy3-labelled secondary antibody, then staining the nuclei with 4'-6-diamidino-2-phenylindole (DAPI), as described (St-Pierre et al., 2002) (Pizzagalli et al., 2003).

Transport assays. The uptake of [6,7-³H]-estrone-3-sulfate (53 Ci/mmol) (NEN Life Science Products, Boston, MA) supplemented with 0.5 µM unlabeled estrone-3-sulfate and [1,2,6,7-³H]-DHEAS (NEN) supplemented with 2 µM unlabeled DHEAS, into stably transfected CHO-K1 cells, was measured in triplicate, as described (Pizzagalli et al., 2003). Specific OATP2B1-mediated uptake was determined by subtracting values generated in CHO-K1 cells transfected with the pcDNA5/FRT vector alone. When comparing the transport activity of wild-type OATP2B1 with the Cys mutants, the variation in expression levels of the proteins was taken into account. The ratio, densitometric units_{mutant}/densitometric units_{OATP2B1}, was used for protein normalization and transport values were calculated as pmol/(mg protein*normalization ratio)*min⁻¹. The kinetics of estrone-3-sulfate uptake at 15 sec by OATP2B1, C493A and C557A, was compared in saturation experiments (0.5 µM to 50 µM). Separate experiments compared the transport of estrone-3-sulfate (at 1 min) by OATP2B1 mutants with and without treatment with thapsigargin to increase surface expression. All Cys mutants were tested for sensitivity to prostaglandin A1,

a cyclopentenone prostaglandin that increases the V_{max} values of OATP2B1 transport (Pizzagalli et al., 2003). Prostaglandin A1 (2 μ M) was added directly to the incubation mixture and uptake values were recorded at 1 min.

Cross-linking of OATP2B1. CHO-K1 cells expressing OATP2B1 (at 80% confluency) were washed with PBS and incubated with 5 mM 3,3'-Dithiobis-[sulfosuccinimidyl-propionate] (DTSSP) or 5 mM (Bis[sulfosuccinimidyl] suberate) BS³ freshly prepared in PBS supplemented with 1 mM MgCl₂ and 0.1 mM CaCl₂ for 60 min at 25°C. The reactions were stopped by washing the cells 3 times with 50 mM Tris/ 150 mM NaCl buffer (pH 7.5). Cells were lysed in buffer (150 mM NaCl, 1mM EDTA, 1% Triton X-100, 10 mM Tris·HCl, pH 7) containing protease inhibitors, and centrifuged for 10 min at 13 000 g at 4°C. The supernatant was divided in two and incubated with or without 20 mM β -mercaptoethanol for 30 min at 4 °C, then mixed and heated (56 °C for 10 min) with Laemmli buffer with or without 142 mM β -mercaptoethanol. Proteins were separated by 6% SDS-PAGE and analysed by Western blotting.

Ni-NTA column purification. His-OATP2B1 was purified on Ni-NTA columns (Qiagen). Crosslinked CHO-K1 cells expressing the HA-OATP2B1 and/or the His-OATP2B1 were washed 3 times with PBS before lysis (50 mM NaH₂PO₄ pH 8, 300 mM NaCl, 10 mM imidazole, 1% Triton, protease inhibitors) at 4°C. Cells were scraped, then centrifuged for 10 min at 13 000 g at 4°C. The supernatant was applied to Ni-NTA columns that had been equilibrated with 600 μ l lysis buffer. The flow-through was collected and the columns were washed four times with 600 μ l of wash buffer (50 mM NaH₂PO₄, 300 mM NaCl, 20 mM imidazole, 1% Triton, pH 8), before elution with 100 μ l of elution buffer (50 mM NaH₂PO₄, 300 mM NaCl, 250 mM imidazole, 1% Triton, pH 8) and analysis by SDS-PAGE and Western blotting. An anti-HA mouse monoclonal antibody (Upstate Biotechnology, Lake

Placidn NY) detected the HA-tagged OATP2B1 and the anti-OATP2B1 antiserum detected total OATP2B1 protein.

RESULTS

Expression of Cys mutants of OATP2B1. CHO-K1 cell lines stably expressed wild-type OATP2B1, the truncated OATP2B1 $_{\Delta 489-557}$ and 10 individual, extracellular Cys to Ala mutations. Expression levels in crude membrane preparations were determined by Western blotting. Compared to the wild-type OATP2B1, which appeared as a 75 kDa band, OATP2B1 $_{\Delta 489-557}$ migrated at the lower molecular weight of 50 kDa, consistent with a truncated OATP2B1 that bears a deletion of 69 amino acids (Fig. 2A). A second prominent band appeared at 105 kDa. The migration patterns of all but one of the single C to A mutants differed from that of wild-type OATP2B1 (Fig. 2A). Mutation of the 1st conserved Cys (C489A) as well as the 3rd (C495A), 4th (C504A), 5th (C516A), 6th (C520A), 7th (C539A), 8th (541A), 9th (C553A) and 10th (C557A), resulted in a major band at approximately 60 kDa, a faint band at the expected 75 kDa, as well as a distinct higher molecular weight species at approximately 180 kDa and in some cases at 150 kDa. Of all mutants, only C493A produced a major band at 75 kDa but unlike OATP2B1, the secondary band at 180 kDa was present. The high molecular weight species were most prominent for mutants C504A, C516A, and C553A. The disappearance of immunoreactivity after adsorption of the antibody with the antigenic peptide confirmed that the additional bands at 60 kDa, 150 kDa and 180 kDa were indeed forms of OATP2B1 (Fig. 2B). Since the stable cell lines were generated using targeted integration of expression vectors, only minor differences in expression levels between OATP2B1 and its variants were expected. Expression levels were determined by adding the densitometric units scanned on Western blots of all band sizes for each OATP2B1 variant. For most mutants, the sum of all bands totaled at least 80% of the level of OATP2B1 wild-type except for C495A and C557A, which were expressed at 50-60% of the

level of OATP2B1 (Fig. 2A). However, repeated measurements showed that the expression level of several mutants relative to wild-type OATP2B1 was labile and could vary 2-fold, primarily as a function of cell density (not shown).

Deglycosylation of OATP2B1. OATP2B1 possesses three consensus sites for N-linked glycosylation (Tamai et al., 2000), only two of which are predicted to be extracellular: Asn 176 in extracellular loop III-IV and Asn 538 in extracellular loop IX-X. OATP2B1 migrated with an apparent molecular weight of 75 kDa on a SDS-PAGE gel. In order to determine whether the Cys mutants that migrated at 60 kDa represent an unglycosylated form, OATP2B1 was deglycosylated with PNGaseF and was incubated with tunicamycin to inhibit its glycosylation. Both treatments yielded a protein that migrated at approximately 55 kDa (Fig. 3). OATP2B1 was insensitive to endoglycosidase H, an enzyme that cleaves only high mannose glycans, as expected for a mature protein undergoing complex glycosylation. Like wild-type OATP2B1, C493A was resistant to endoglycosidase H but sensitive to PNGaseF (Fig. 3). C489A, C495A, C504A, C516A, C520A and C539A were partially sensitive to PNGase F as well as to endoglycosidase H and showed small downward shifts from approximately 60 kDa to 55 kDa, as expected for immature proteins that undergo core-glycosylation rather than full complex glycosylation. C541A, C553A and C557A underwent thermal aggregation during the extended incubation times required for enzymatic deglycosylation (not shown).

Transport activity of OATP2B1 mutants. To determine whether the mutation of external Cys residues altered the function of OATP2B1, the transport of estrone-3-sulfate by the Cys mutants was compared to OATP2B1 (Fig. 4A). C493A achieved 60% and C557A achieved 30% of the transport rate of OATP2B1, whereas the activity of all other mutants decreased by 85% or more (Fig. 4A). When the protein expression was normalized for the amount of OATP2B1 calculated by densitometry, only the transport rate of C557A increased

significantly to 60% of the rate of OATP2B1 (Fig. 4A). The kinetics of estrone-3-sulfate transport by OATP2B1, C493A and C557A was compared (Fig. 4B). The estimated K_m value was lowest for OATP2B1 ($4.1 \pm 2.7 \mu\text{M}$) compared to $18.0 \pm 7.2 \mu\text{M}$ for C493A and $7.2 \pm 8.2 \mu\text{M}$ for C557A and the estimated V_{max} (pmol/normalized mg·min⁻¹) value was highest for OATP2B1 (1941 ± 327) compared to C493A and C557A (1085 ± 167 and 567 ± 250 , respectively). The transport of DHEAS was severely reduced (by 80% and 50% for C493A and C557A, respectively) and kinetic parameters could not be estimated reliably (Fig. 5)

Confocal Microscopy. In order to determine whether the impaired transport by OATP2B1 mutants was due to mistargeting, all transfected cell lines were examined by confocal microscopy. OATP2B1 and C493A were expressed at the plasma membrane with occasional intracellular staining, whereas the truncated OATP2B1_{Δ489-557} was sequestered intracellularly (Fig 6). All other mutants showed predominant cytoplasmic staining with varying extents of membrane staining, indicating that mutant proteins failed to mature and reach the cell surface. Since immature proteins retained intracellularly do not undergo complete glycosylation, this explains the predominant band at 60 kDa for all C to A substitutions except C493A, rather than the expected band at 75 kDa (Fig. 2, Fig. 3).

Rescue of OATP2B1 Cys mutants. The intracellular localization of mutant proteins prevented a thorough assessment of the structure-function relationship of the individual Cys residues. In order to induce expression at the cell surface, the Cys mutants were rescued by treating the cells with thapsigargin, a Ca²⁺-ATPase inhibitor that interferes with the interaction of chaperone proteins and newly synthesized proteins in the endoplasmic reticulum (Egan et al., 2002). Cell-surface biotinylation with the membrane-impermeant biotinylation reagent, NHS-SS-biotin, was used to quantify the surface expression of each Cys mutant. In experiments without thapsigargin, 80% of total OATP2B1 was biotinylated

at the cell surface and this did not change with thapsigargin treatment (Table 1; Fig. 6). In the case of C493A, 78% of total reached the surface both in the presence and absence of thapsigargin and consisted of both the 75 kDa and 180 kDa species, indicating that C493A exists in two forms at the plasma membrane (Fig. 7; Table 1). The cell surface expression of all other Cys mutants was variable, ranging from approximately 18% for C553A to 58% for C504A (Table 1) with both the 60 kDa and 180 kDa forms at the cell surface in the absence of thapsigargin (Fig. 7A). Thapsigargin promoted the disappearance of the core-glycosylated 60 kDa form, and the appearances of the 75 kDa and 180 kDa forms at the cell surface (Fig. 7C). Thapsigargin treatment did not change the extent of cell surface expression of C504A (Table 1) but did increase the surface delivery for C489A, C495A, C516A, C520A, C539A, C541A, C553A and C557A (Table 1). The ER resident protein, BiP, appeared at 75 kDa on immunoblots of total lysates (Fig. 7B, 7D) but was absent from immunoblots of avidin-biotin pull-down lysates (Fig. 7A, 7C), confirming that intracellular proteins did not contaminate the assay. The increase in cell surface expression was also evident after confocal microscopy where more immunostaining was present at the plasma membrane after exposure to thapsigargin (Fig. 6B). The immunostaining of OATP2B1 and C493A was not different after thapsigargin treatment (not shown).

Transport activity of rescued OATP2B1 Cys mutants. In order to determine whether the poor transport activity of several Cys mutants reflected a genuine decrease in function or rather the intracellular sequestration of the proteins, the transport assays were repeated after treatment with thapsigargin (Table 1; Fig. 4C). For C489A, C495A, C516A, C520A, C539A and C541A, the uptake of estrone-3-sulfate increased slightly after thapsigargin treatment, commensurate with the increase in cell surface expression (Table 1). There was no change in the activity of C504A, consistent with its lack of response to thapsigargin rescue. Surprisingly, the activity of C553A decreased despite a modest increase in surface

expression. The effect of thapsigargin on the kinetic parameters of transport was considered by repeating the saturation experiments for estrone-3-sulfate in pre-treated OATP2B1 and C557A expressing cells (Fig. 4C). A 3 to 4-fold increase in both K_m and V_{max} was observed for both OATP2B1 and C557A.

We have shown previously that the naturally occurring cyclopentenone prostaglandins A1 and A2 increased the estimated V_{max} of OATP2B1 in kinetic experiments with estrone-3-sulfate or DHEAS, (Pizzagalli et al., 2003). The activity of all thapsigargin-rescued Cys mutants was tested in the presence of PGA1 to determine whether individual Cys residues were sensitive to its action. The uptake of estrone-3-sulfate was increased 1.5 to 3-fold in all cases, indicating that Cys residues in the extracellular loop were not involved in the action of PGA1 (Fig. 8).

Disulfide bond formation in OATP2B1. After incubation with thapsigargin to induce cell surface expression of the Cys mutants, cells expressing OATP2B1 and its Cys variants were exposed to MTSEA-biotin, a membrane-impermeable, thiol-reactive agent. Disulfide-bonded and free cysteines can be distinguished by treatment with MTSEA-biotin because only free cysteines will form a mixed disulfide with this alkylthiosulfonate and be detected on immunoblots of avidin-biotin pull-down assays. OATP2B1 did not react with MTSEA-biotin at the cell surface, indicating that the extracellular cysteines were not free (Fig. 9A). All OATP2B1 Cys mutants at the cell surface did react with MTSEA-biotin and were detected on immunoblots of lysates after avidin-biotin pull-down reactions, primarily as the 180 kDa form (Fig. 9A). This suggests that individual substitution of any one of the ten extracellular Cys residues resulted in a free cysteine residue available to interact with MTSEA-biotin. When cells were incubated with MTSEA-biotin without prior thapsigargin treatment, faint bands appeared at 60 kDa and 180 kDa but not at 75 kDa (Fig. 9B). The

corresponding immunoblots of total cell lysate with thapsigargin (Fig. 9C) confirmed the partial rescue of mutants by the appearance of the 75 kDa form.

Cross-linking of OATP2B1. Cross-linking experiments were designed in order to determine whether OATP2B1 itself could adopt a high molecular weight conformation, but one that did not survive the conditions of denaturing SDS-PAGE. The membrane-impermeant, thiol-cleavable, cross-linking agent DTSSP, enables cross-linking of amino groups up to 12 Å, and the non-cleavable agent, BS³, cross-links amino groups 11.4 Å apart. Cell surface OATP2B1 was cross-linked by both agents and appeared on immunoblots at the monomeric size of 75 kDa and at the 150 kDa dimeric size (Fig. 10). The reducing agent β-mercaptoethanol was able to cleave the DTSSP cross-linked OATP2B1 back to its monomeric size. By comparison, the mutant protein C541A, migrated slightly slower than cross-linked OATP2B1.

To confirm that cross-linked OATP2B1 formed homodimers rather than a stoichiometric interaction with another protein, the cross-linking experiments were repeated in cells expressing HA tagged and/or His tagged OATP2B1. HA-OATP2B1 alone appeared in the flow-through fraction of Ni-NTA columns, but bound and eluted from columns as a dimeric 150 kDa protein when crosslinked with BS³ in doubly transfected HA/His-OATP2B1 expressing cells (Fig. 11A). Complete cross-linking was never achieved, which accounts for the additional monomeric 75 kDa HA-tagged protein appearing in the flow-through of HA/His-OATP2B1 expressing cells. When the crosslinking was performed with DTSSP but cleaved with β-mercaptoethanol before the Ni-NTA column purification, monomeric HA-OATP2B1 appeared in the flow-through (Fig. 11B).

Because the expression level of several mutant proteins proved more labile than that of wild-type OATP2B1, we examined whether the Cys mutants were subject to a more rapid

degradation. Cultured cells were incubated for 15 h with the proteasome inhibitors, N-acetyl-L-leucyl-L-leucyl-L-norleucinal (ALLN) (50 μ M) and lactacystin (20 μ M) and cell lysates were analyzed by SDS-PAGE and Western blotting. The protein levels of wild-type OATP2B1 were not affected by ALLN (Fig. 12) or lactacystin (not shown), whereas those of C489A, C495A and to a less extent C493A, were increased by both inhibitors (Fig. 12). Moreover, treatment with ALLN and lactacystin favored the accumulation of aggregated forms of the proteins at 180 kDa and even at 250 kDa.

DISCUSSION

We explored the structure-function relationship of the ten conserved cysteine residues in loop IX-X of OATP2B1. The intracellular sequestration of OATP2B1 $_{\Delta 489-557}$ shows that the loop is necessary for surface expression of OATP2B1. Our findings also show that: 1) all extracellular cysteines in loop IX-X, except for C493, are necessary for targeting of OATP2B1 to the cell surface and that thapsigargin can partially rescue the mistargeted mutants; 2) despite rescue, substitution of C489, C495, C504, C516, C520, C539, C541 and C553 impairs transport function; 3) substitutions at C493 and C557 partially conserve transport; 4) all ten extracellular cysteines are likely involved in disulfide linkages.

Except for C493A, the targeting defect of the Cys mutants can be ascribed to protein misfolding. Misfolded proteins trapped in the ER undergo only core glycosylation (Fig. 2, 3), are prone to aggregation when overexpressed (Johnston et al., 1998) and are subjected to proteasomal degradation (Gong et al., 2005). The discreet bands at 150 and 180 kDa on immunoblots likely represent complexes of misfolded proteins, since they proved refractory to detergents and denaturants and accumulated when degradation by the proteasome was inhibited (Figs. 2, 7, 12). Moreover, the sulfhydryl reagent, N-ethylmaleimide, or reducing

agents did not prevent aggregation, indicating that the spurious formation of non-native disulfide bonds did not mediate this process (not shown). Molecular chaperones associate with misfolded proteins to prevent delivery to the plasma membrane (Ellgaard and Helenius, 2003). This association can be disturbed by depleting the ER calcium stores with sarcoplasmic reticulum Ca^{2+} ATPase pump inhibitors, thereby rescuing the mutant protein from intracellular sequestration and promoting its maturation (Egan et al., 2002). Thapsigargin and curcumin have been used to this effect with variable success (Egan et al., 2002) (Loo et al., 2004). In the present experiments, thapsigargin but not curcumin, increased the surface expression of 8 out of 9 immature mutants with variable efficacy (Table 1), consistent with an upward shift from 60 kDa to 75 kDa on SDS-PAGE (Fig. 7) and greater plasma membrane immunostaining (Fig. 6). Delisle *et al.* studied the rescue of a series of mutant K^+ channels and reported similar variability (Delisle et al., 2003). In a series of mutant glycoprotein hormone receptors, Mizrachi *et al.* noted that the distinct conformation adopted by any given mutant could result in the recruitment of different chaperones (Mizrachi and Segaloff, 2004) and such differences in chaperone protein associations in this series of OATP2B1 mutants may have been a determinant of the extent of thapsigargin rescue.

We reasoned that even partial correction of the mistargeting of mutants would provide a means of distinguishing between impaired uptake of estrone-3-sulfate due to failure to reach the cell surface and that due to a non-functioning protein. Despite thapsigargin treatment, C489A, C495A, C504A, C516A, C520A, C539A, C553A and C541A remained severely impaired (Table 1, Fig. 8), indicating that modifications of these 8 residues were incompatible with the binding and/or transport. These 8 mutants appeared at the cell surface predominantly as the 180 kDa form (Fig. 7C) and it could be argued that this represents an incompetent protein complex and that the substitution of Cys with the nonpolar residue Ala

generated transport-defective OATP2B1 variants solely because of an increased propensity of these more hydrophobic mutants to form complexes. The behaviour of C493A tends to support this notion since C493A underwent normal targeting but transported less efficiently than OATP2B1 ($V_{max}/K_m = 60$ vs. $473 \mu\text{l}/\text{normalized } \mu\text{g protein}\cdot\text{min}^{-1}$ for C493A and OATP2B1, respectively) (Fig. 4B). However, C489A, C495A, C516A, C539A and C541A did show increased transport after thapsigargin rescue when a higher fraction of the protein at the cell surface consisted of the 180 kDa form (Fig. 7C, Table 1), indicating that this form was likely functional in some cases. The thapsigargin treatment itself was not detrimental to transport function, because the 2 - 4-fold increase in both K_m and V_{max} for OATP2B1 and C557A (Fig. 4C) preserved the overall efficiency of transport. However, a thapsigargin-induced disruption of chaperone protein associations is not expected to be completely silent. The OATP2B1 variants may have adopted different conformations in the presence and absence of chaperone proteins, which may explain the changes in the kinetic parameters (Fig. 4C) and the decrease in C553A activity (Table 1).

The tendency for the Cys mutants to form 180 kDa complexes and the fact that members of other 12 transmembrane domain transporters, such as the Na^+/Cl^- -dependent neurotransmitter transporter family, undergo oligomerization (Just et al., 2004) (Hastrup et al., 2001), prompted us to investigate whether OATP2B1 self-associated under native conditions. BS³ and DTSSP cross-linked OATP2B1 appeared as homodimers of 150 kDa, which indicates the potential for inter-molecular contacts between lysines that are up to 12 Å apart (Figs. 10, 11). Lysines residing in extracellular loops I-II, III-IV, V-VI and VII-VIII are obvious candidates for this interaction. However, due caution must be exercised before inferring that homodimerization represents a relevant quaternary structure of OATP2B1. Protein overexpression may have promoted the capture of dimerization by cross-linking and detection by complementary immunological methods is mandatory.

Intramolecular disulfide bond formation is favored in the oxidizing extracellular and ER compartments and there are examples of disulfide loss causing mistargeting or malfunction of receptors and transporters (Tarnow et al., 2003). The reactivity of MSTEA-biotin with all mutants but not with wild-type OATP2B1, is consistent with the notion that a free unpaired thiol was generated after each C to A substitution and that all ten conserved cysteines in the extracellular loop IX-X of OATP2B1 are normally disulfide linked (Fig. 9A). Substitution of C489, C495, C517, C539 and C541, and presumably their respective disulfide bonding, were the most functionally debilitating. Since the presumed bonding involving either Cys493 or Cys557 was less critical for function, it is tempting to assign a disulfide linkage between C493 and C557. However, consideration must also be given to C465, predicted to be at the interface of transmembrane helix IX and extracellular loop IX-X and to two cysteines residing in extracellular loop X-XI, which are also conserved among OATP/Oatp members and may interact with the ten cysteines studied here.

A cyclopentenone prostaglandin stimulated estrone-3-sulfate transport in this series of mutants (Fig. 8). We had postulated previously (Pizzagalli et al., 2003) that the mechanism of action may involve a covalent reaction between the electrophilic prostaglandin and susceptible cysteine residues in OATP2B1, as shown for I-kappa- β kinase and thioredoxin reductase (Moos et al., 2003). We were unable to detect covalent binding of biotinylated prostaglandin A1 with OATP2B1 in immunoprecipitation experiments (not shown). Since CHO-K1 express endogenous Mrp1 and both estrone-3-sulfate (Nunoya et al., 2003) and the glutathione conjugate of prostaglandin A1 are substrates for Mrp1, an indirect mechanism must be considered whereby the efflux of estrone-3-sulfate by Mrp1 is inhibited. Two findings argue against the effect being solely due to inhibition of Mrp1: 1) prostaglandin A1 was able to stimulate estrone-3-sulfate uptake in the presence of the Mrp1 inhibitor, indomethacin 10 μ M; and 2) pretreatment of cells with buthionine sulfoximine to reduce

glutathione, thereby affecting both the formation of prostaglandin A1-GSH and the efflux of estrone-3-sulfate (Nunoya et al., 2003), did not prevent the stimulation. Although the mechanism of prostaglandin A1 stimulation is unknown, it clearly does not involve any of the 10 cysteine residues in extracellular loop IX-X.

Glycosylation itself has been shown to affect the function of rat *Oatp1a1* (gene symbol *Slco1a1*), a protein with four confirmed glycosylation sites, one of which is in extracellular loop IX-X (Lee et al., 2003). Whereas the mutation of any single *Oatp1a1* glycosylation site did not critically affect function, mutating two or more glycosylation sites did impair function and lead to an inactive, mistargeted protein that failed to reach the cell surface. Whether glycosylation of OATP2B1 is necessary for activity is unknown and it is possible that the loss of function experienced by the Cys mutants is secondary to incomplete glycosylation. However, this could only partially explain the functional consequences of Cys substitutions because thapsigargin did increase the appearance of the glycosylated forms in all cases (Fig. 7C, D) and yet C4553A and C520A did not respond accordingly with an increase in function (Table 1).

Given that the extracellular loop IX-X is a common structural motif of all OATP/Oatps, our observations may apply to other members of the OATP superfamily. OATP1B3 exists as a polymorphic variant that carries a Gly to Cys mutation at position 522 (OATP1B3-G522C) within extracellular loop IX-X (Letschert et al., 2004). Compared to the wild-type OATP1B3, OATP1B3-G522C was mistargeted when expressed in a MDCK cell line and was unable to transport the bile acid, cholytaurine (Letschert et al., 2004). OATP1B1 also has polymorphic variants within extracellular loop IX-X and one of these, OATP1B1-G488A, shows impaired transport activity and reduced surface expression when transfected into HeLa cells (Tirona et al., 2001). This suggests that other OATPs with

polymorphisms or modifications in their large extracellular loop IX-X may be vulnerable to functional impairment.

Acknowledgements

We are grateful for the help provided by Dr. M. Hoechli and the use of the facilities of the Electron Microscopy Laboratory, University of Zürich, Switzerland.

References

Delisle BP, Anderson CL, Balijepalli RC, Anson BD, Kamp TJ and January CT (2003) Thapsigargin selectively rescues the trafficking defective LQT2 channels G601S and F805C. *J Biol Chem* **278**:35749-38754.

Egan ME, Glockner-Pagel J, Ambrose C, Cahill PA, Pappoe L, Balamuth N, Cho E, Canny S, Wagner CA, Geibel J and Caplan MJ (2002) Calcium-pump inhibitors induce functional surface expression of Delta F508-CFTR protein in cystic fibrosis epithelial cells. *Nat Med* **8**:485-492.

Ellgaard L and Helenius A (2003) Quality control in the endoplasmic reticulum. *Nat Rev Mol Cell Biol* **4**:181-191.

Gao B, Huber RD, Wenzel A, Vavricka SR, Ismail MG, Reme C and Meier PJ (2005) Localization of organic anion transporting polypeptides in the rat and human ciliary body epithelium. *Exp Eye Res* **80**:61-72.

Gong Q, Keeney DR, Molinari M and Zhou Z (2005) Degradation of trafficking-defective long QT syndrome type II mutant channels by the ubiquitin-proteasome pathway. *J Biol Chem* **280**:19419-19425.

Hagenbuch B and Meier PJ (2004) Organic anion transporting polypeptides of the OATP/ SLC21 family: phylogenetic classification as OATP/ SLCO superfamily, new nomenclature and molecular/functional properties. *Pflugers Arch - Eur J Physiol* **447**:653-665.

Hastrup H, Karlin A and Javitch JA (2001) Symmetrical dimer of the human dopamine transporter revealed by cross-linking Cys-306 at the extracellular end of the sixth transmembrane segment. *Proc Natl Acad Sci U S A* **98**:10055-10060.

Horton RM, Ho SN, Pullen JK, Hunt HD, Cai Z and Pease LR (1993) Gene splicing by overlap extension. *Methods Enzymol* **217**:270-279.

Johnston JA, Ward CL and Kopito RR (1998) Aggresomes: a cellular response to misfolded proteins. *J Cell Biol* **143**:1883-98.

Just H, Sitte HH, Schmid JA, Freissmuth M and Kudlacek O (2004) Identification of an additional interaction domain in transmembrane domains 11 and 12 that supports oligomer formation in the human serotonin transporter. *J Biol Chem* **279**:6650-6657.

Kobayashi D, Nozawa T, Imai K, Nezu J, Tsuji A and Tamai I (2003) Involvement of human organic anion transporting polypeptide OATP-B (SLC21A9) in pH-dependent transport across intestinal apical membrane. *J Pharmacol Exp Ther* **306**:703-708.

Kullak-Ublick GA, Ismail MG, Stieger B, Landmann L, Huber R, Pizzagalli F, Fattinger K, Meier PJ and Hagenbuch B (2001) Organic anion-transporting polypeptide B (OATP-B) and its functional comparison with three other OATPs of human liver. *Gastroenterology* **120**:525-33.

Lee TK, Koh AS, Cui Z, Pierce RH and Ballatori N (2003) N-glycosylation controls functional activity of Oatp1, an organic anion transporter. *Am J Physiol Gastrointest Liver Physiol* **285**:G371-G381.

Letschert K, Keppler D and Konig J (2004) Mutations in the SLCO1B3 gene affecting the substrate specificity of the hepatocellular uptake transporter OATP1B3 (OATP8). *Pharmacogenetics* **14**:441-452.

Loo TW, Bartlett MC and Clarke DM (2004) Thapsigargin or curcumin does not promote maturation of processing mutants of the ABC transporters, CFTR, and P-glycoprotein. *Biochem Biophys Res Commun* **325**:580-585.

Mizrachi D and Segaloff DL (2004) Intracellularly located misfolded glycoprotein hormone receptors associate with different chaperone proteins than their cognate wild-type receptors. *Mol Endocrinol* **18**:1768-1777.

Moos PJ, Edes K, Cassidy P, Massuda E and Fitzpatrick FA (2003) Electrophilic prostaglandins and lipid aldehydes repress redox-sensitive transcription factors p53 and hypoxia-inducible factor by impairing the selenoprotein thioredoxin reductase. *J Biol Chem* **278**:745-750.

Nozawa T, Imai K, Nezu J, Tsuji A and Tamai I (2004) Functional characterization of pH-sensitive organic anion transporting polypeptide OATP-B in human. *J Pharmacol Exp Ther* **308**:438-445.

Nunoya K, Grant CE, Zhang D, Cole SP and Deeley RG (2003) Molecular cloning and pharmacological characterization of rat multidrug resistance protein 1 (mrp1). *Drug Metab Dispos* **31**:1016-1026.

Pizzagalli F, Varga Z, Huber RD, Folkers G, Meier PJ and St-Pierre MV (2003) Identification of steroid sulfate transport processes in the human mammary gland. *J Clin Endocrinol Metab* **88**:3902-3912.

Satoh H, Yamashita F, Tsujimoto M, Murakami H, Koyabu N, Ohtani H and Sawada Y (2005) Citrus juices inhibit the function of human organic anion-transporting polypeptide OATP-B. *Drug Metab Dispos* **33**:518-523.

St-Pierre MV, Hagenbuch B, Ugele B, Meier PJ and Stallmach T (2002) Characterization of an Organic Anion Transporting Polypeptide OATP B in Human Placenta. *J Clin Endocrin Metab* **87**:1856-1863.

Tamai I, Nezu J, Uchino H, Sai Y, Oku A, Shimane M and Tsuji A (2000) Molecular identification and characterization of novel members of the human organic anion transporter (OATP) family. *Biochem Biophys Res Commun* **273**:251-260.

Tarnow P, Schoneberg T, Krude H, Gruters A and Biebermann H (2003) Mutationally induced disulfide bond formation within the third extracellular loop causes melanocortin 4 receptor inactivation in patients with obesity. *J Biol Chem* **278**:48666-48673.

Tirona RG, Leake BF, Merino G and Kim RB (2001) Polymorphisms in OATP-C: identification of multiple allelic variants associated with altered transport activity among European- and African-Americans. *J Biol Chem* **276**:35669-35675.

Footnotes

* This work was supported by a grant from the University of Zürich Forschungskommission 2003 (to M.V. St-Pierre) and grants from the National Science Foundation, Switzerland (3100-67173) to M.V. St-Pierre and 31-64140 to P.J. Meier.

¹ Contributed equally to this work

.

FIGURE LEGENDS

Fig. 1. Two-dimensional representation of the extracellular IX-X loop of OATP2B1 showing the relative positions of the ten conserved cysteines (C) and one N-glycosylation site.

Fig. 2. Expression of wild-type OATP2B1 and Cys mutant in CHO-K1 cells. OATP2B1, the truncated OATP2B1 $\Delta_{489-557}$ and individual Cys to Ala mutant proteins were separated by SDS-PAGE and analysed by Western blotting. Blots were probed with a polyclonal OATP2B1 antibody in the absence (A) or presence (B) of 3 mM antigenic peptide. 70 μ g of crude membrane proteins were applied to each lane. pcDNA5, vector control lacking insert.

Fig. 3. Analysis of N-linked glycosylation of OATP2B1 and its variants. Membrane proteins (35 μ g) were treated with peptide N-glycosidase F (PNGase F) or endoglycosidase H (Endo H) under denaturing conditions to remove N-linked oligosaccharides and analyzed by SDS-page and Western blotting. Untreated membranes were incubated with denaturing buffers without enzymes. OATP2B1 and C493A were sensitive to PNGase F and shifted downwards from 75 kDa to approximately 55 kDa but were resistant to Endo H. Tunicamycin treatment to inhibit glycosylation also produced a band at 55 kDa. Mutants, C489A, C495A, C504A, C516A, C520A and C539A migrated at approximately 60 kDa in control reactions but shifted downwards after treatment with EndoH. Mutants showed partial sensitivity to PNGase F.

Fig. 4. Transport characteristics of wild-type and mutant OATP2B1. (A) Uptake of [3 H]-estrone-3-sulfate (0.5 μ M) at 1 min was determined by subtracting values generated in control CHO-K1 cells transfected with pcDNA5/FRT. Values are expressed as a percentage of the uptake measured for wild-type OATP2B1 (black bars). To account for the differences in OATP2B1 protein expression between stable transfectants, densitometric measurements were made on Western blots. Values were calculated as $\text{pmol}/(\text{mg protein} \times \text{normalization ratio}) \times \text{min}^{-1}$, where normalization ratio =

densitometric units_{mutant}/densitometric units_{OATP2B1} and values are reported as percentage of the uptake in wild-type OATP2B1 (white bars). Measurements are in triplicate \pm SD.

(B) Saturation curve of [³H]-estrone sulfate (E₁S) uptake in OATP2B1 (■) and mutants C493A (○), and C557A (▼). Uptake was determined by subtracting values obtained in cells transfected with the pcDNA5/FRT vector alone. Protein expression was normalized as described in (A) using densitometric measurements of Western blots shown in the right panel. Values are the mean of triplicates \pm SD. The Michaelis-Menten equation was fit to the data using nonlinear regression. The estimated K_ms (μM) were 4.2 ± 2.7 for OATP2B1, 18.0 ± 7.2 for C493A and 7.2 ± 7 for C557A.

(C) Saturation curve of [³H]-estrone sulfate (E₁S) in OATP2B1 (■) and mutant C557A (▼) expressing cells pre-treated with thapsigargin to increase surface expression. Values obtained in cells transfected with the pcDNA5/FRT vector alone were subtracted. Protein expression (shown in the Western blots in the right panel) was normalized for the level of OATP2B1 in untreated cells (right panel B), as described in 4A. Values are mean of triplicates \pm SD. The estimated K_ms (μM) obtained from curve fitting the Michaelis Menten equation were 15.0 ± 3.8 for OATP2B1 and 13.4 ± 11.0 for C557A.

Fig. 5. Transport of [³H]-DHEAS (2 μM) in OATP2B1, C493A and C557A expressing CHO-K1 cell. Uptake was measured at 1 min and values are reported as percentage of the uptake measured for wild-type OATP2B1 after subtracting the values generated in control cells transfected with pcDNA5/FRT (black bars). Values were also calculated as pmol/(mg protein*normalization ratio)*min⁻¹, where normalization ratio = densitometric units_{mutant}/densitometric units_{OATP2B1}, to account for differences in expression. Normalized values are also reported as percentage of the uptake in wild-type OATP2B1 (white bars). Measurements are in triplicate \pm SD.

Fig. 6. Immunofluorescent detection of OATP2B1 and mutant proteins expressed in CHO-K1 cells. Cells were incubated with a polyclonal rabbit anti-OATP2B1 antibody and with a secondary Cy3-conjugated anti-rabbit IgG antibody and examined by confocal microscopy. Nuclei were stained with

DAPI (blue). **(A)** Wild-type OATP2B1 and C493A are expressed in the plasma membrane of CHO-K1 cells. The truncated mutant lacking all ten extracellular cysteines (OATP2B1 $\Delta_{489-557}$) and the other nine Cys to Ala mutants show primarily an intracellular localization. **(B)** After pre-treatment with thapsigargin, immunostaining is also detected at the plasma membrane for mutants protein that localized intracellularly in panel A.

Fig. 7. Total and cell surface expression of wild-type and mutant OATP2B1 using Sulfo-NHS-LC-Biotin. **(A)** Immunoblot of Sulfo-NHS-biotin labeled surface proteins from non-thapsigargin treated cells probed with OATP2B1 antibody. **(B)** Western blot of total lysates (surface and intracellular proteins) from non-thapsigargin treated cells. **(C)** Same procedure as in **(A)** but cells were pretreated with thapsigargin. **(D)** Same as in **(B)** but with thapsigargin treatment. For all samples, 5 μ l of the lysate were loaded onto 7.5% SDS-PAGE gels and detected with the anti-OATP2B1 antibody. The bottom panel in **(A)**, **(B)**, **(C)** and **(D)** show the immunodetection of BiP at 75 kDa. BiP was not detected at the cell surface in **(A)** and **(C)** but was present in total lysates **(B)** and **(D)**.

Fig 8. Effect of prostaglandin A1 on wild-type and mutant OATP2B1 mediated [6,7- 3 H]-estrone sulfate (E_1S) uptake. Cells were retreated with thapsigargin to promote expression at the cell surface. Uptake values were determined by subtracting values generated in pcDNA5/FRT vector control cells in the absence (black bars) and presence of prostaglandin A1 (2 μ M) (open bars). Prostaglandin A1 stimulated the uptake by OATP2B1 and all Cys mutants. Data are reported as mean \pm SD of triplicate measurements.

Fig. 9. Detection of free cysteines in WT and mutant OATP2B1 with MTSEA-biotin. **(A)** Following thapsigargin treatment, MTSEA-biotin labeled cell surface proteins were lysed, pulled down with neutravidin beads, subjected to SDS-PAGE (40 μ l) and to subsequent Western blot analysis with OATP2B1 antibody. **(C)** Western blotting of total lysates (surface and intracellular protein (10 μ l)) from which pull downs were performed. **(B)** Same procedure as in **(A)** but cells were not pretreated

with thapsigargin. **(D)** Western blotting of total lysates as in **(C)** but without thapsigargin pretreatment.

Fig. 10. Cross-linking of OATP2B1. CHO-K1 cells expressing OATP2B1 were incubated with 5 mM thiol-cleavable 3,3'-Dithiobis-[sulfosuccinimidylpropionate] (DTSSP) (lanes 3 and 4) or with 5mM (Bis[sulfosuccinimidyl] suberate) (BS³) (lanes 5 and 6) for 60 min at 25°C. Cells lysates were separated by 6% SDS-PAGE and analysed by Western blotting. Samples in lanes 2, 4 and 6 were treated for 30 min at 4 °C with 20 mM β-mercaptoethanol (β-ME) and with 142 mM β-ME in the sample buffer. Samples in lanes 1, 3 and 5 were not exposed to reducing agent. Lanes 7 and 8: Mutant C541A without (lane 7) and with thapsigargin pre-treatment (lane 8).

Fig. 11 Cross-linking of HA tagged and His tagged OATP2B1. CHO-K1 cells expressing either His-OATP2B1 and/or HA-OATP2B1 were crosslinked with 5mM (Bis[sulfosuccinimidyl] suberate) (BS³) for 60 min at 25°C. Cells lysates were loaded onto Ni-NTA purification columns to bind the 6x His tag. Flow-throughs (FT) and eluates (E) were separated by 6% SDS-PAGE and analysed by Western blotting. **(A)** Detection with an anti-HA antibody confirms that HA-OATP2B1 is cross-linked with His-OATP2B1. **(B)** His-OATP2B1 and HA-OATP2B1 co-expressing cells were treated with 5 mM thiol-cleavable 3,3'-Dithiobis-[sulfosuccinimidylpropionate] (DTSSP) then exposed to reducing agent (20 mM β-ME). The cells lysate was loaded on a Ni-NTA purification column and analyzed by Western blotting with an anti-HA antibody. HA-OATP2B1 was detected only in the flow-through. **(C)** Western blot of samples shown in **(A)** detected with a rabbit anti-OATP2B1 antibody.

Fig. 12 Effect of proteasome inhibitors on expression of OATP2B1 and its variants. CHO-K1 cells expressing wild-type OATP2B1, C489A, C493A or C495A were exposed for 15h to 50 μM N-acetyl-L-leucyl-L-leucyl-L-norleucinal (+ ALLN) or 20 μM lactacystin (+ Lac) or were untreated (-). Cell lysates were separated by 7.5% SDS-PAGE and analyzed by Western blotting with a rabbit anti-OATP2B1 antibody.

Table 1

Rescue of mistargeted mutant OATP2B1 proteins by thapsigargin

Protein	<i>Surface expression</i> ^a			<i>E₁S uptake after thapsigargin</i> ^e
	<i>- thapsigargin</i>	<i>+ thapsigargin</i>		
	(%)	(%)	(<i>fold-change</i>)	(<i>fold-change</i>)
OATP2B1	80 (76, 84)^b	76 ± 1.8^c	0.95	0.99 ± 0.17
C489A	55 (54, 56)	76^d	1.38	1.83 ± 0.35
C493A	78 (85, 72)	77	0.99	1.02 ± 0.12
C495A	23 (30, 17)	58	2.52	2.54 ± 0.31
C504A	58	57	0.98	1.00 ± 0.18
C516A	32 (44, 20)	55 (51, 59)	1.72	2.33 ± 0.56
C520A	51	72	1.41	1.17 ± 0.20
C539A	40 (50, 30)	68 (58, 78)	1.70	2.92 ± 0.92
C541A	28 (24, 32)	61 (52, 70)	2.18	2.92 ± 0.21
C553A	18 (19,16)	47 (50, 44)	2.61	0.52 ± 0.95
C557A	35 (31, 40)	57 (58, 56)	1.63	1.10 ± 0.09

^a calculated as the ratio of biotinylated OATP2B1/mutants pulled-down by neutravidin to the total in cellular lysates, as measured by densitometric analyses of immunoblots.

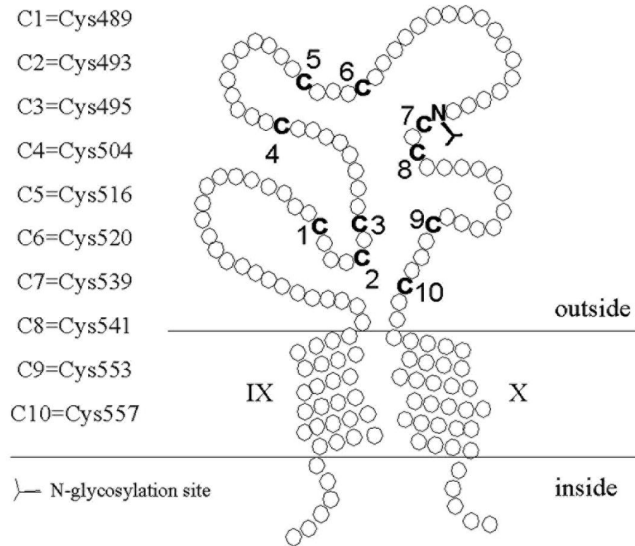
^b mean of duplicates with individual values given in parentheses

^c mean of triplicate

^d single experiments

^e calculated as the ratio of estrone-3-sulfate uptake in cells pretreated with thapsigargin to non-treated cells (n = 3)

Fig.1



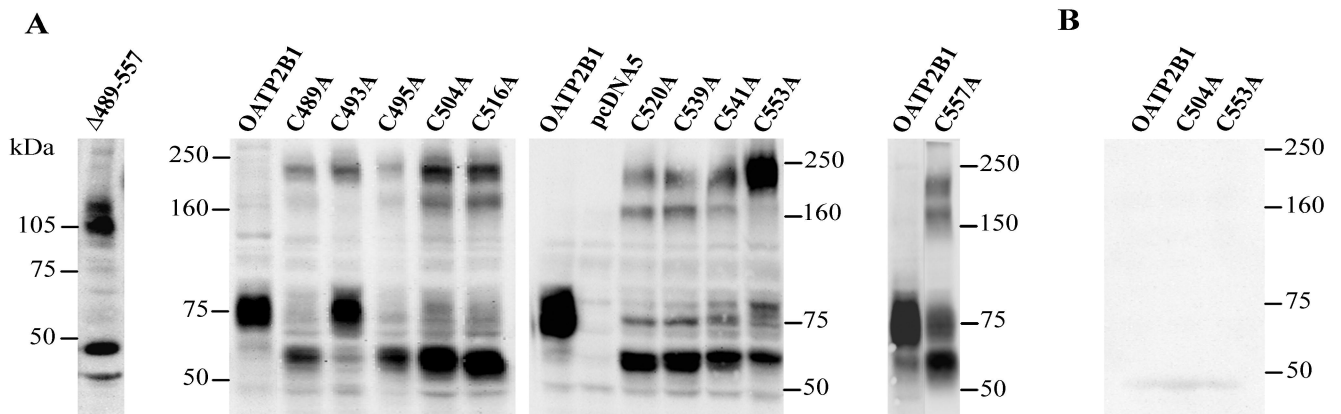


Figure 3

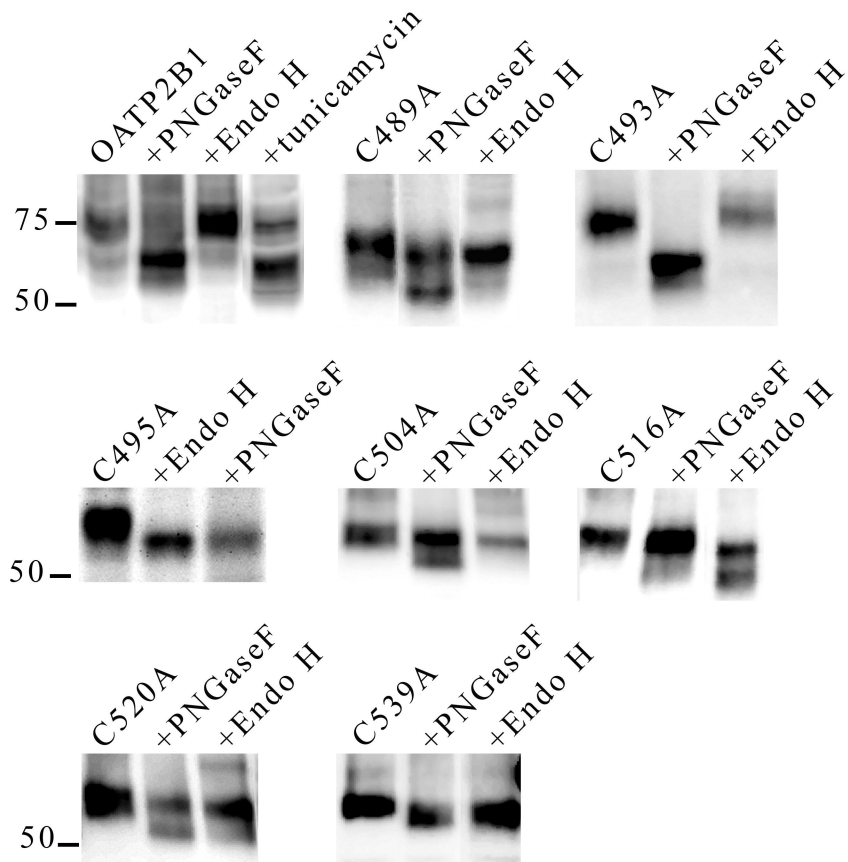


Fig.4

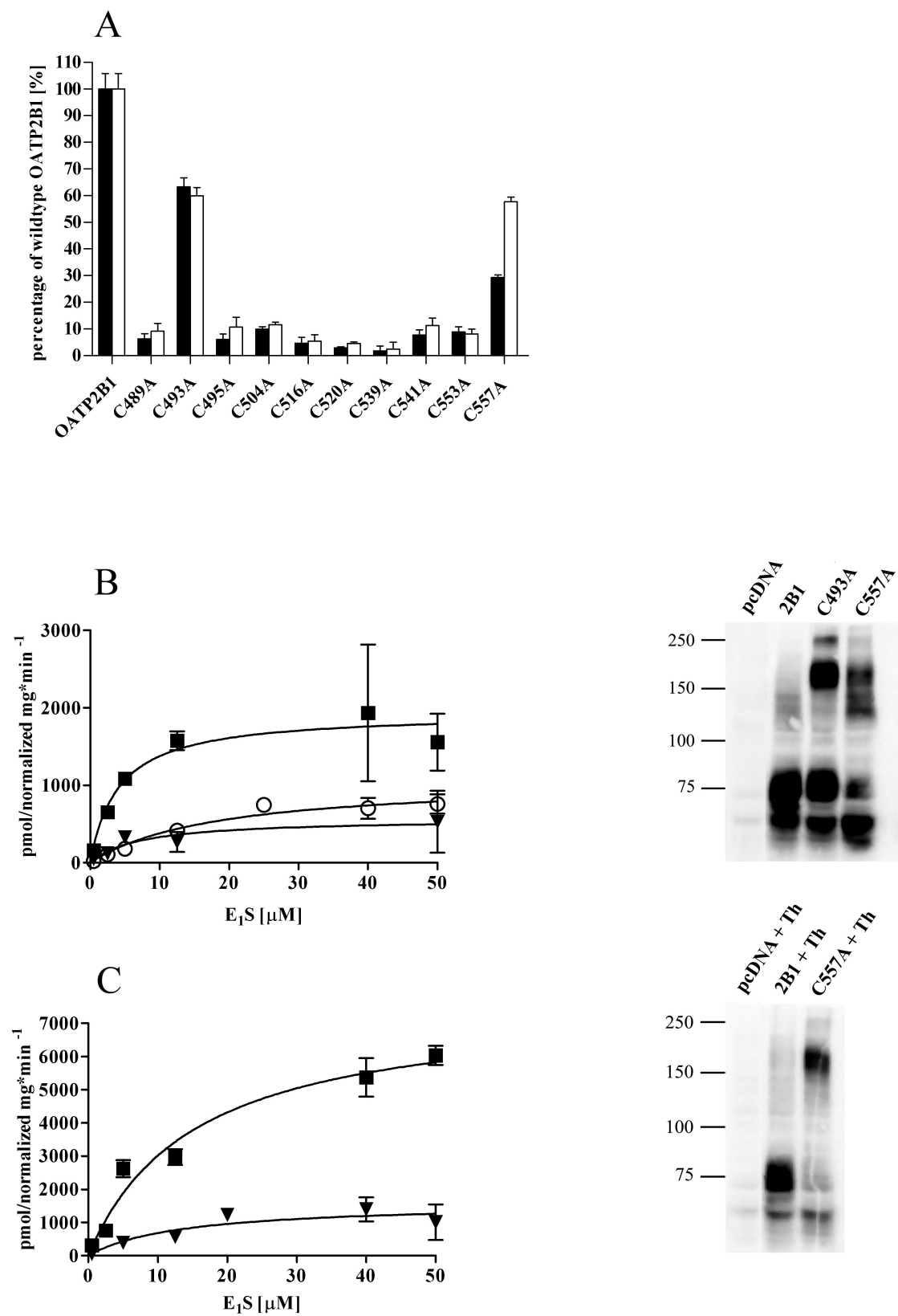


Fig.5

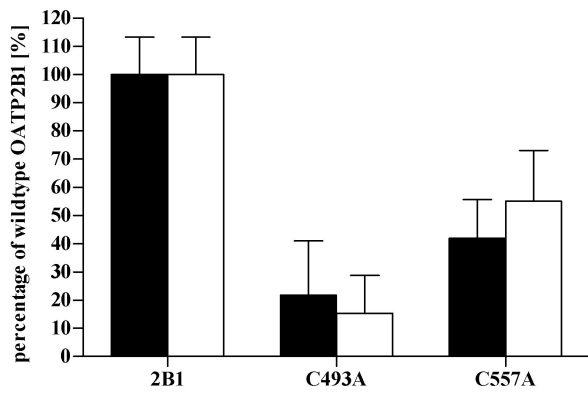
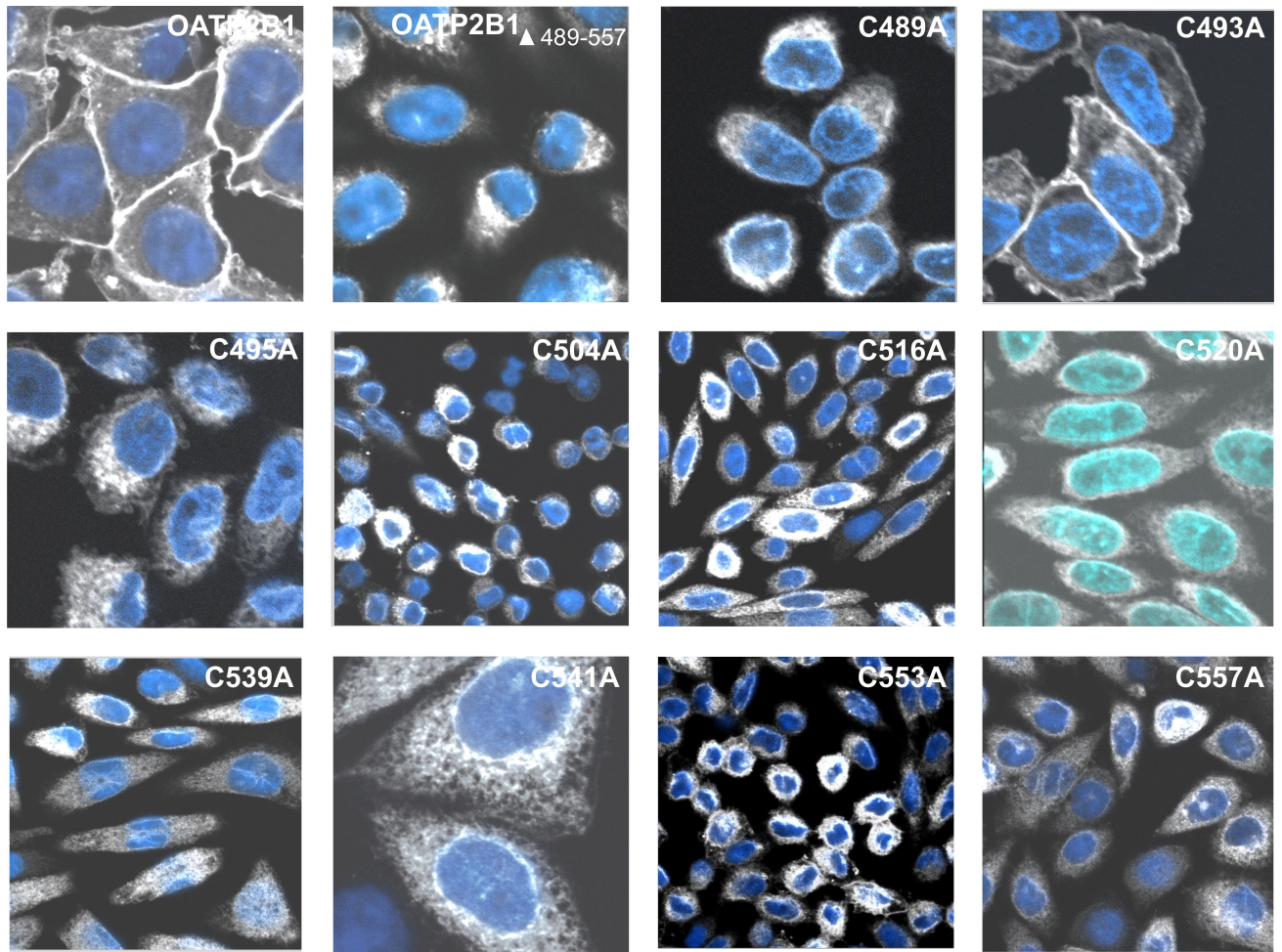


Figure 6

A



B

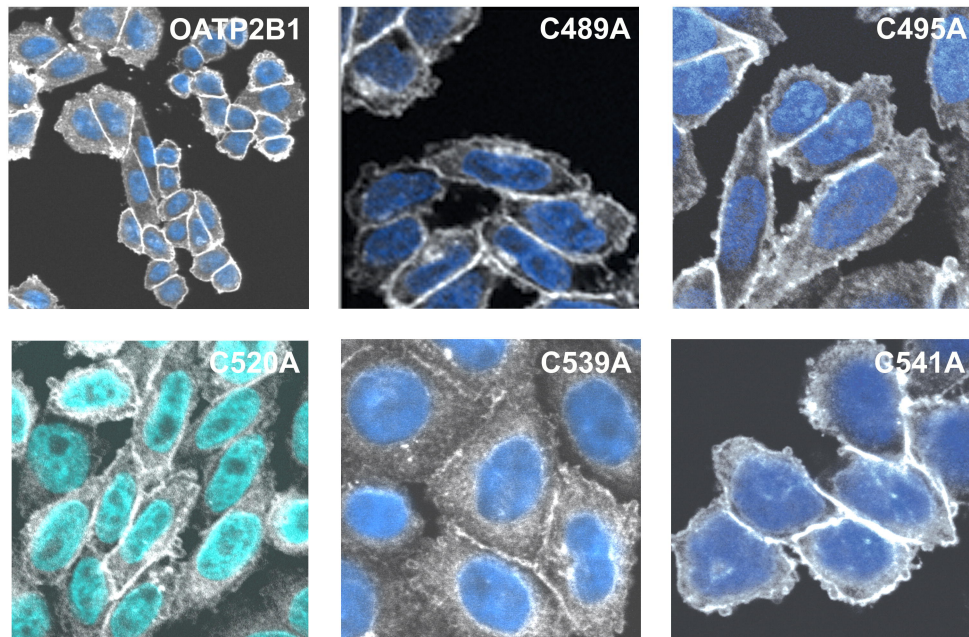
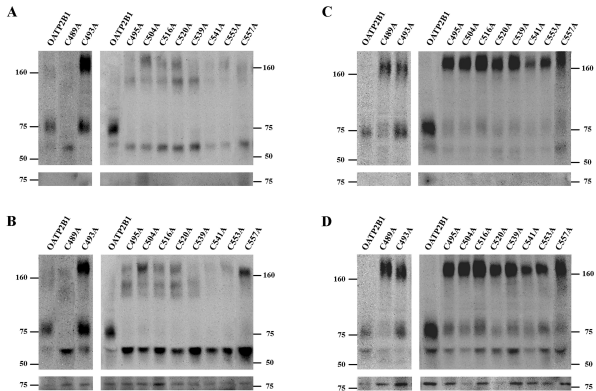


Figure 7



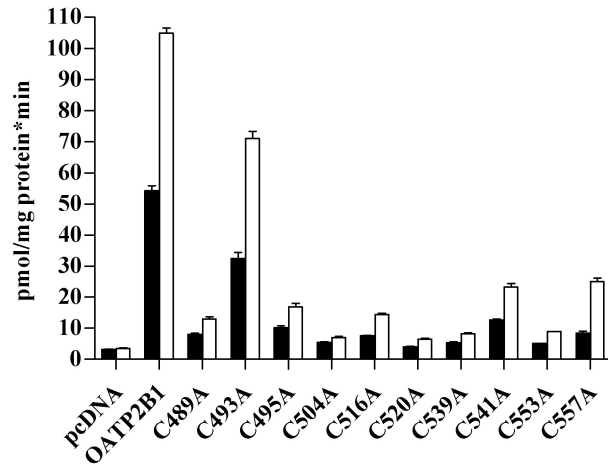


Fig. 8

Fig. 9

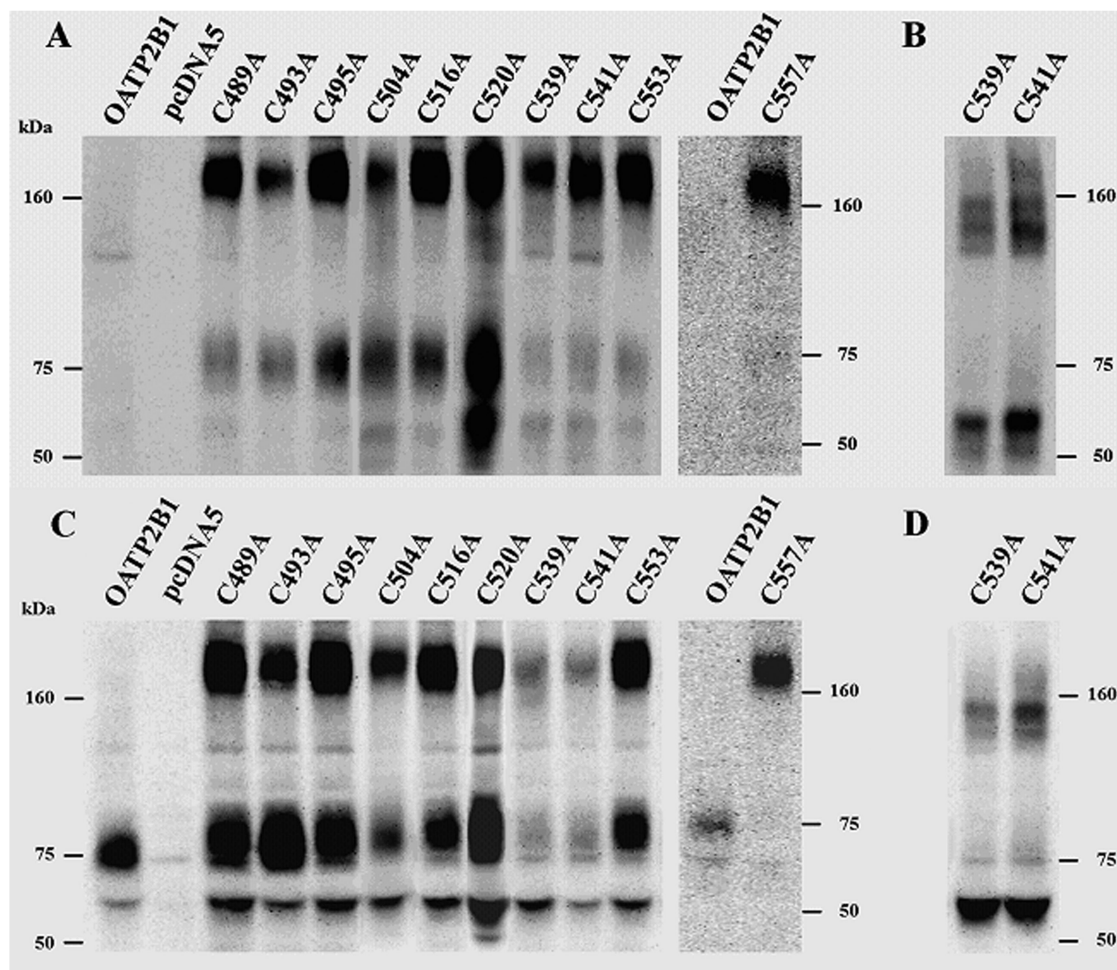


Figure 10

BS ³	-	-	-	-	+	+
DTSSP	-	-	+	+	-	-
β-ME	-	+	-	+	-	+

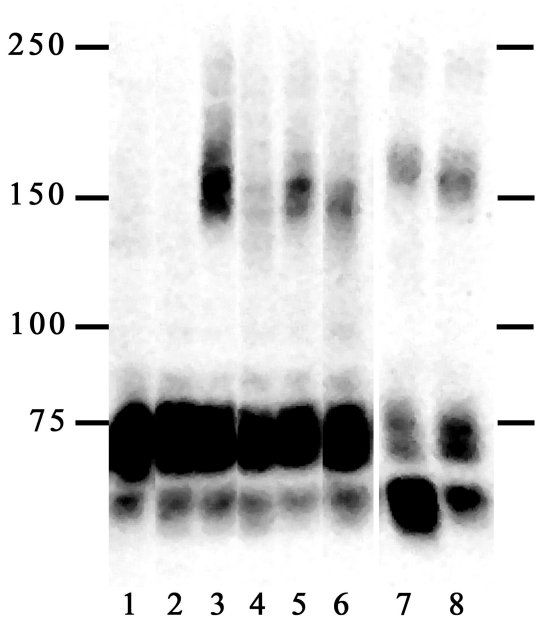


Fig. 11

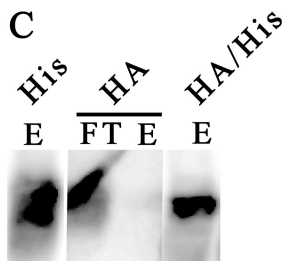
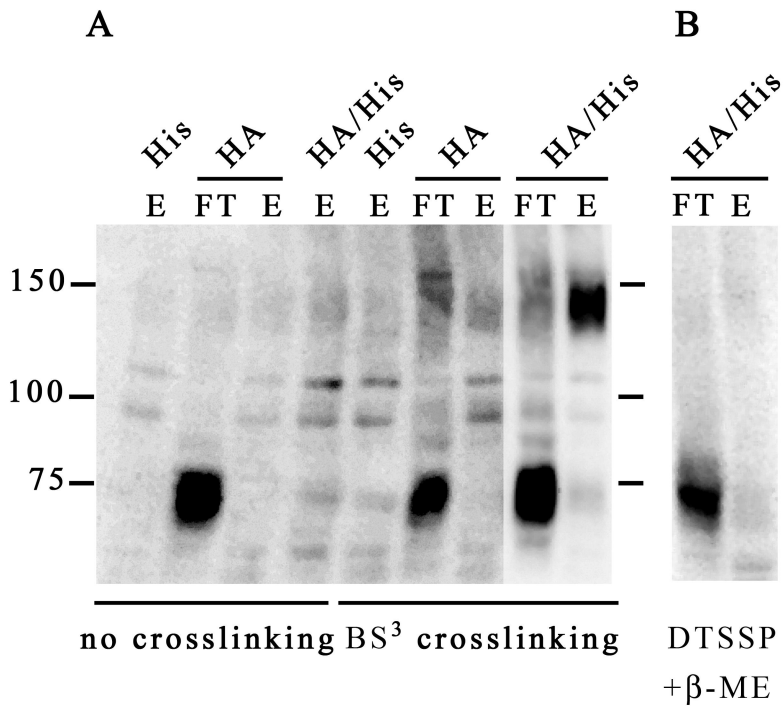


Fig.12

